

USING IMAGE ANALYSIS TO LOOK INTO THE EFFECT OF IMPURITY CONCENTRATION IN NaCl CRYSTALLIZATION

A. FERREIRA¹, N. FARIA¹, F. ROCHA^{1,*}, S. FEYO DE AZEVEDO¹ and A. LOPES²

¹Faculdade de Engenharia da Universidade do Porto, Portugal

²Departamento de Química, Universidade da Beira Interior, Portugal

This paper presents and describes a methodology for morphology assessment, crystal particle classification and quantification of the complexity level of a crystal or a population of crystals. It further describes the application of such methodology to the study of the influence of MgCl₂ in the crystallization of NaCl, namely on crystal size and morphology. Image analysis techniques are combined with discriminant factorial analysis leading to results that allow the computation of the complexity of crystals through a new parameter, the agglomeration degree of crystals. With this methodology it has been possible to distinguish automatically among three different classes of crystals, and within each class as per their complexity. Agreement between manual and automated classification measured in terms of a performance index is 90% on average. The effect of supersaturation and impurity concentration on the type, amount and complexity level of the agglomerates was further determined.

Keywords: crystal morphology; agglomeration; impurities; sodium chloride.

INTRODUCTION

Crystallization is a widely implemented process in the chemical industry production and purification stages of particulate products. Though a generally efficient process for purification, it is often a complex operation mainly due to the difficulty in obtaining reliable experimental data related to the properties of the particulate solid systems.

An image analysis technique, developed by Pons *et al.* (1997, 1998) and adapted to the study of sucrose crystallization by Faria *et al.* (Faria *et al.*, 2003; Feyo de Azevedo *et al.*, 2002), has proved to be very effective in the quantification of crystal size and morphology distributions. In the present work this technique is extended and applied to the NaCl/MgCl₂/H₂O system, aiming at quantifying the influence of impurity (MgCl₂) concentration in the size distribution and agglomeration phenomena.

The distinction between agglomeration and other similar phenomena, as aggregation and flocculation, is important but also very difficult (Mullin, 1992). According to Hartel *et al.* (1988), agglomeration is the unification of primary particles that are cemented by chemical bonds. Depending on the type of inter-particle forces, three categories of

agglomeration processes may be distinguished (Mersmann, 1994):

- If the cohesion forces are weak, such as van der Waals forces (Schubert, 1981), the agglomeration is called flocculation.
- If, in supersaturated systems, the agglomerating crystals stick strongly together, for example through a crystalline bridge, the process is called agglomeration.
- For intermediary processes and for processes arising without supersaturation, the phenomenon is usually referred to as aggregation.

During a crystallization process agglomeration usually occurs when the system is supersaturated, whereas aggregation occurs in saturated or under-saturated solutions (Mersmann, 1994). A further distinction can be made between two types of crystal agglomeration: (a) primary agglomeration as a result of malgrowth of crystals (polycrystals, dendrites, and twins), and (b) secondary agglomeration as a consequence of crystal-crystal collisions in supersaturated solutions (Mersmann, 1994).

Though very relevant to the study of crystallization kinetics and crystal morphology, knowledge of agglomeration phenomena is still today relatively scarce, due to the difficulty in measuring and quantifying those phenomena and their effects in the particle populations. In this work, a methodology and an image analysis technique are proposed that address and deal with such problems.

*Correspondence to: Dr F. Rocha, Departamento de Engenharia Química, Faculdade de Engenharia da Universidade do Porto, Rua Roberto Frias, 4200-465 Porto, Portugal.
E-mail: frocha@fe.up.pt

EXPERIMENTAL PROCEDURE

The crystallization experiments were carried out in a fluidized bed crystallizer. The crystallization plant used is constructed of glass with a total capacity of about 25 L (Figure 1). This apparatus consists essentially of a stock vessel (20 L), which contains the mother liquor, three heat exchangers (P1, P2 and P3) to help in controlling the supersaturation, and a fluidized bed crystallizer, CR.

The mother liquor leaving the stock vessel circulates through three heat exchangers before entering the fluidized bed crystallizer. At the top and bottom of the crystallizer there is a thin net to enclose the seeds.

The temperature of the solution in the stock vessel is usually kept at about 10 to 15°C higher than its saturation point in order to dissolve any secondary nuclei. Type K thermocouples located at both ends of the crystallizer and connected to an ECD Model 50 Datalogger allow continuous, on line, monitoring of the temperature. All experiments were performed at 30°C. The crystallizer is charged with 3–4 g of seed crystals. The crystals are then allowed to grow during a controlled time of around 5 minutes. Porosity (ϵ) is kept constant at 0.9, regulated by the valve V5. After each run, the crystals are washed, dried and re-weighed.

Experimental runs were carried out for two different concentrations of MgCl_2 in the mother-liquor, respectively 47.6 and 95.2 g of MgCl_2 per kilogram of water. These solutions were prepared using analytical grade sodium chloride and magnesium chloride hexa-hydrated (Merck p.a., 99.5%) and deionized water with a conductivity of $2 \mu\text{s cm}^{-1}$.

NaCl seed crystals, with a mean size of 530 μm , were obtained by sieving the commercial Merck salt.

The supersaturation of this system was measured with a doped polypyrrole electrode. This electrode, doped with NaCl, was prepared by electrochemical polymerization from a solution containing 0.1 M of pyrrole and 0.1 M of NaCl in deionized water. The preparation was carried out using a platinum disc working electrode with an area of 0.03 cm^2 , a Calomel saturated reference electrode and a platinum wire auxiliary electrode. The polymerization took place for 1 hour under an applied potential of 1 V.

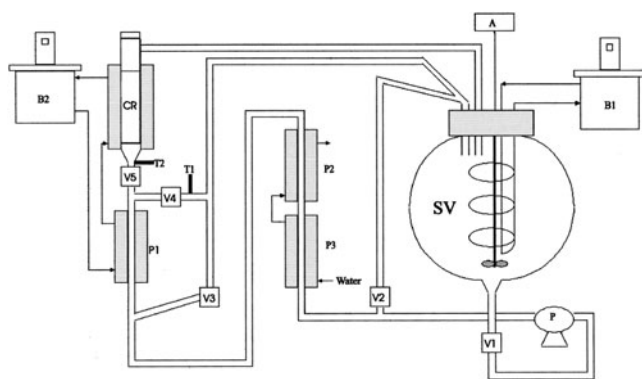


Figure 1. Experimental apparatus. SV, Stock vessel; P1, P2 and P3, heat exchangers; CR, fluidized bed crystallizer; B1 and B2, thermostatic baths; A, agitator; V1, V2, V3, V4 and V5, valves; P, pump; T1 and T2, thermocouples.

The determination of the concentrations using the polypyrrole electrode, as well as the preparation of the calibration curve, were all made at constant temperature (298 K) (Ferreira and Lopes, 2002).

Crystal growth rate, R_g , was related with the initial and final mass of the crystals, M_i and M_f respectively, through the following equation

$$R_g = \frac{3K_v\rho_c L_i}{K_a\Delta\theta} \left[\left(\frac{M_f}{M_i} \right)^{1/3} - 1 \right] \quad (1)$$

where $\Delta\theta$ is the run duration, ρ_c is the sodium chloride density (2.163 kg m^{-3}) (Perry and Green, 1984), K_v and K_a are the volume and surface shape factors for the cubic crystals of NaCl, which take the values 1 and 6 respectively, and L_i is the seed mean size ($5.30 \times 10^{-4} \text{ m}$). The measured rates were correlated with the thermodynamic driving force, $\Delta\mu/RT$, according to

$$R_g = k_G \left(\frac{\Delta\mu}{RT} \right)^g \quad (2)$$

where k_G is the growth rate constant and g the overall growth order. The driving force, $\Delta\mu/RT$, was defined in terms of mean ionic activities, a , as:

$$\frac{\Delta\mu}{RT} = \ln \frac{a_s}{a^*} = \ln \frac{\gamma_s m_s}{\gamma^* m^*} \quad (3)$$

where the indices * and s refer to the saturated and super-saturated solutions, respectively, γ is the activity coefficient and m is the molality. The activity coefficients were calculated by the Pitzer molal ion-interaction model (Pitzer, 1995) which for the ternary system $\text{NaCl}/\text{MgCl}_2/\text{H}_2\text{O}$ takes the form:

$$\begin{aligned} \ln \gamma_{\pm \text{NaCl}} = & f^\gamma + (m_{\text{Na}} + m_{\text{Cl}}) \left(B_{\text{NaCl}} + \frac{Z}{2} C_{\text{NaCl}} \right) \\ & + m_{\text{Mg}} \left(B_{\text{MgCl}} + \frac{Z}{2} C_{\text{MgCl}} + \Phi_{\text{NaMg}} \right) \\ & + m_{\text{Cl}} (m_{\text{Na}} C_{\text{NaCl}} + m_{\text{Mg}} C_{\text{MgCl}}) \\ & + m_{\text{Mg}} m_{\text{Cl}} \frac{\Psi_{\text{NaMgCl}}}{2} + \frac{1}{2} m_{\text{Na}} m_{\text{Mg}} \Psi_{\text{NaMgCl}} \\ & + m_{\text{Na}} m_{\text{Cl}} \frac{\partial B_{\text{NaCl}}}{\partial I} + m_{\text{Mg}} m_{\text{Cl}} \frac{\partial B_{\text{MgCl}}}{\partial I} \\ & + m_{\text{Na}} m_{\text{Mg}} \frac{\partial \Phi_{\text{NaMg}}}{\partial I} \end{aligned} \quad (4)$$

with

$$f^\gamma = -A^\phi \left[\frac{I^{1/2}}{1 + bI^{1/2}} \right] + \frac{2}{b} \ln(1 + bI^{1/2}) \quad (5)$$

$$Z = \sum_i m_i |z_i| \quad (6)$$

where A^ϕ is the Debye-Hückel parameter, I the ionic strength, $b = 1.2 \text{ kg}^{1/2} \text{ mol}^{-1/2}$, m the molality, z the atomic number of specie i , B and C the second and third

Virial term for pure electrolytes, and Φ and Ψ the second and third Virial term for mixed electrolytes.

The parameters used in equation (4) were obtained from the literature, according to Puthela *et al.* (1987).

The NaCl solubility values used in this work are published in Ferreira and Lopes (2002) and are presented in Figure 2.

MORPHOLOGY ASSESSMENT AND CLASSIFICATION

Image Analysis

The crystals are deposited on a glass slide and observed by transmitted light microscopy (Leica DMLB) with a monochrome camera (Leica DC 100) connected to a PC, where eight-bit grey-level images of 768×576 square pixels are captured. These images (about 220 per sample, which correspond to 400–500 crystals) are then treated, analysed and several numerical descriptors are extracted for each crystal using *VisilogTM5* (Noesis, les Ulis, France).

Before performing the measurements, the image treatment, consists of: reduction of the colour depth of the image from 256 levels of grey to two colours, hole filling, noise elimination, elimination of the objects that contact the board of the image and identification of the particles in the image (Faria *et al.*, 2003). The image descriptors are silhouette surface S from which the equivalent diameter ($D_{eq} = 2\sqrt{S/\pi}$) is deduced, perimeter P , number of internal zones N (Faria *et al.*, 2003), Feret diameters distribution, from which the maximal (F_{max}) and minimal (F_{min}) are deduced (Figure 3). These Feret diameters are calculated at different angles α , with the diameter being the distance between two parallel tangents to the silhouette and making an angle α with the vertical. From these parameters a set of secondary parameters are calculated: (i) circularity $C = P^2/(4\pi S)$; (ii) elongation (F_{max}/F_{min}); (iii) aspect ratio (F_{max}/D_{eq}); (iv) *areas_{ratio}* (S/S_{in}), where S_{in} is the surface occupied by the internal zones, the central and transparent parts of the crystal (Figure 3); (v) *box_{ratio}* (S_{box}/S), where $S_{box} = F_{min}(\alpha) \cdot F_{min}(\alpha + 90^\circ)$; (vi) the particle robustness (Ω_1), its index of largest concavity (Ω_2), the ratio of the largest concavity to the total concavity (Ω_3) (Pons *et al.*, 1997).

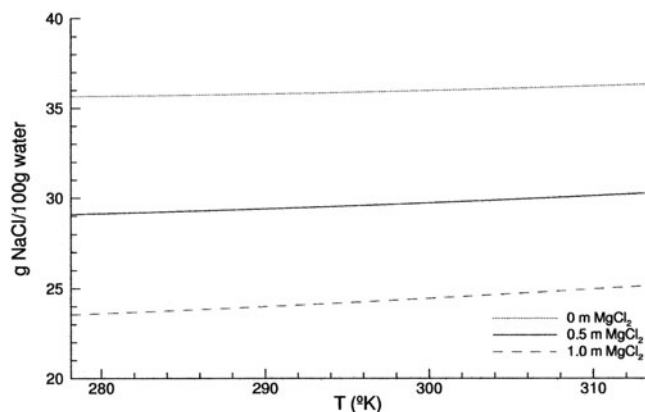


Figure 2. Solubility of NaCl at different impurity concentrations (Ferreira and Lopes, 2002).

Crystal Classification

Crystals are separated in seven groups that should represent different (increasing) types of complexity. In this work, as shown in Figure 4, such grouping results from a first distinction between simple crystals and agglomerates, the latter being further distinguished, depending on inter-particle bonds that occur during this crystallization process, between type A agglomerates and type B agglomerates. Type A agglomerates are, apparently, crystals with primary agglomeration. Type B agglomerates seem to show secondary agglomeration resulting of crystal–crystal collisions.

Agglomerates belonging to type A are further separated into three sub-groups according to the degree of complexity of their projected image: small (Sa), medium (Ma), and large (La). As for type B crystals, they are separated as sub-type Ka, Kb and Kc, also according to the complexity of their projected silhouette.

Using the parameters obtained from the image analysis, applied to a population test of 800 crystals visually classified by an operator, three discriminant factorial analysis (DFA) methods were trained. The first one performs the distinction among simple crystals, type A agglomerates and type B agglomerates. The second one further classifies type A agglomerates as Sa, Ma and La. As for the third DFA method, it classifies type B crystals as Ka, Kb and Kc.

The trained algorithms are then used to automatically classify the crystals obtained from the experiments. A statistical toolbox, XLstat (T. Fahmy, Paris, France), running under Excel (Microsoft) was used for this purpose.

The degree of mismatch between the automated and visual classifications is evaluated by the following performance index

$$PI (\%) = \left(1 - \frac{\text{Number of misclassified crystals}}{\text{Total number of crystals}} \right) \times 100 \quad (7)$$

The performance indexes for the automated classification are shown in Table 1. These were obtained using the parameters: *Box_{ratio}*, *Areas_{ratio}*, F_{max}/F_{min} , F_{max}/D_{eq} , Ω_1 , Ω_2 , Ω_3 , N and Feret diameters. The performance indexes for the distinction among simple crystals, type A, and type B agglomerates are very high (around 90%). This reveals a high agreement between the automated and visual classifications.

On the other hand, the classification agreement for the agglomerates sub-classes is not so good, which reveals the

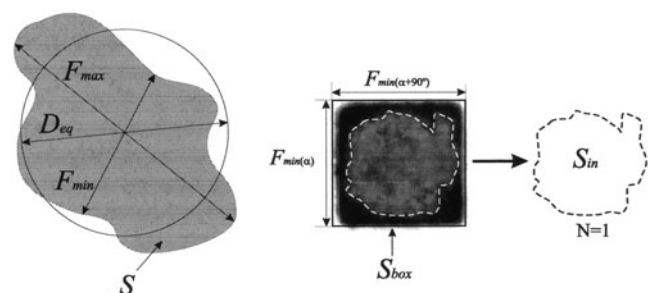


Figure 3. Image analysis parameters.

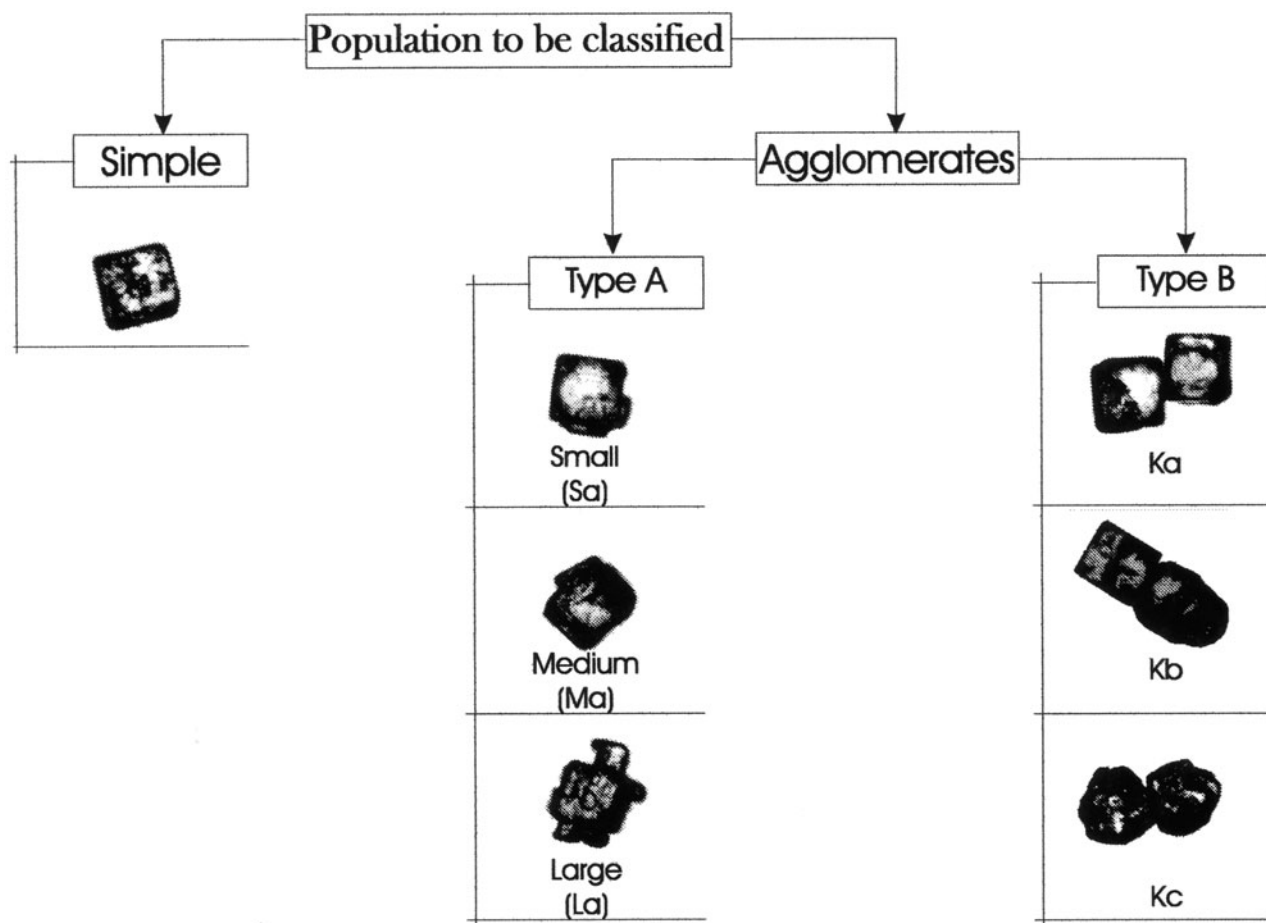


Figure 4. Classification tree for NaCl crystals.

higher subjectivity level of this latter type of classification. Nevertheless, excluding the sub-class Ma and Kb, it is a meaningful result of the method developed as it conveys a measurement of the complexity of the agglomerates.

Quantifying Agglomeration

The DFA method used to classify the crystals gives the probability of each crystal belonging to each of the groups considered. Using these probabilities, it is possible

Table 1. Classification performance index.

	PI %
Simple	90.6
Type A	86.7
Type B	97.5
Ka	65.2
Kb	58.7
Kc	71.9
Sa	65.0
Ma	55.0
La	82.0

to calculate one parameter representing the complexity of the crystal.

Each crystal of the entire population is first classified as simple, type A agglomerates, or type B agglomerates. From this classification, one obtains three probabilities of each crystal i belonging to each one of the three groups ($Pb_{i,S}$, $Pb_{i,A}$ and $Pb_{i,B}$).

All crystals classified as type A agglomerates are further classified according to their degree of complexity, namely as Sa, Ma or La. Thus we obtain the three probabilities of each type A crystal i belonging to each one of these three classes ($Pb_{i,Sa}$, $Pb_{i,Ma}$ and $Pb_{i,La}$).

The crystals classified as type B agglomerates are similarly further classified into three groups of growing complexity (Ka, Kb and Kc), from which three new probabilities result ($Pb_{i,Ka}$, $Pb_{i,Kb}$ and $Pb_{i,Kc}$).

Combining all these probabilities into one single parameter, it is possible to obtain a simple measure of the crystal complexity. Faria *et al.* (2003) proposed a new parameter, the agglomeration degree of a crystal, Ag_i , that characterises the degree of complexity of a crystal by a linear combination of the probabilities of occurrence of four types of crystals. This method is now adapted to this new situation where the crystals are previously separated into three different classes and then, for each one of the two agglomerate types found they are classified into three new classes according to their complexity. What is

looked at in the present work is an expression of the degree of agglomeration of a crystal that is a function of the probabilities of belonging to the classes, taking the form:

$$Ag_i = [Pb_{i,S} + Pb_{i,A}(C_1Pb_{i,Sa} + C_2Pb_{i,Ma} + C_3Pb_{i,La}) + Pb_{i,B}(C_1Pb_{i,Ka} + C_2Pb_{i,Kb} + C_3Pb_{i,Kc}) - 1] \times 100 \quad (8)$$

The relevant parameters, C_1 , C_2 and C_3 , of this new non-linear combination are identified from the following set of restrictions

$$Pb_{i,S} + Pb_{i,A} + Pb_{i,B} = 1 \quad (9)$$

$$Pb_{i,Sa} + Pb_{i,Ma} + Pb_{i,La} = 1 \quad (10)$$

$$Pb_{i,Ka} + Pb_{i,Kb} + Pb_{i,Kc} = 1 \quad (11)$$

and criteria for levels of aggregation:

$$Pb_{i,S} = 1 \Rightarrow Ag_i = 0 \quad (12)$$

$$Pb_{i,A} = 1 \Rightarrow \begin{cases} Pb_{i,Sa} = 1 \Rightarrow Ag_i = 33.(3)\% \\ Pb_{i,Ma} = 1 \Rightarrow Ag_i = 66.(6)\% \\ Pb_{i,La} = 1 \Rightarrow Ag_i = 100\% \end{cases} \quad (13)$$

$$Pb_{i,B} = 1 \Rightarrow \begin{cases} Pb_{i,Ka} = 1 \Rightarrow Ag_i = 33.(3)\% \\ Pb_{i,Kb} = 1 \Rightarrow Ag_i = 66.(6)\% \\ Pb_{i,Kc} = 1 \Rightarrow Ag_i = 100\% \end{cases} \quad (14)$$

From such conditions, the following expression results for the agglomeration degree.

$$Ag_i = \left[Pb_{i,S} + Pb_{i,A} \left(\frac{4}{3}Pb_{i,Sa} + \frac{5}{3}Pb_{i,Ma} + 2Pb_{i,La} \right) + Pb_{i,B} \left(\frac{4}{3}Pb_{i,Ka} + \frac{5}{3}Pb_{i,Kb} + 2Pb_{i,Kc} \right) - 1 \right] \times 100 \quad (15)$$

RESULTS AND DISCUSSION

The experimental procedures previously described were used to evaluate the effect of $MgCl_2$, in a concentration of 0.5 m (mol solute/kg solvent) or 1 m, on the NaCl crystallization process. This work focused on the effect of this impurity on the crystal growth rate and agglomeration degree. The image analysis is based on direct measurements of the different dimensions and characteristics that may identify a certain particle, namely the agglomeration degree and the kind of agglomerate. In this section the experimental results referring to the overall growth rate and the properties of the crystal populations are presented.

Crystallization Experiments

The results referring to NaCl crystallization at different impurity concentrations are published in Ferreira and Lopes (2002) and are presented in Figure 5.

The impurity makes the growth rate order to increase slightly, from 1.89 to 1.97. However this parameter remains unchanged for the two impurity concentrations used.

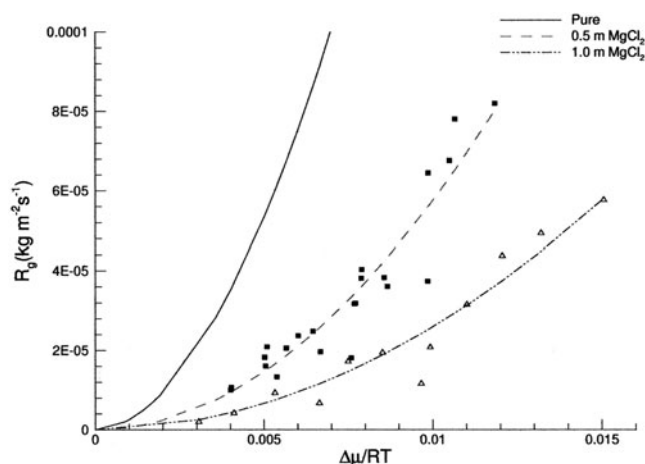


Figure 5. Growth rate of NaCl in pure mother liquors and in ternary solutions with $MgCl_2$ ($\epsilon = 0.9$) (Ferreira and Lopes, 2002).

The growth rate constant, k_G , decreases with the increase of the impurity concentration (Table 2).

Image Analysis Results

Applying the previously described image analysis technique to this system, it is possible to measure a set of crystal properties that identify the population. This was done for all experiments. Table 3 shows an example of the results obtained.

The size distribution is divided in three size classes: small crystals [<0.55 mm], medium crystals [$0.55-0.70$ mm] and large crystals [>0.70 mm]. The composition according to the crystal classification (simple, type A agglomerates and type B agglomerates) given by image analysis, for each of these size classes, can be made. In Figure 6 is presented an example, for an $MgCl_2$ concentration of 0.5 m and $\Delta\mu/RT = 1.375 \times 10^{-3}$. It can be seen that the small crystals are essentially simple and type A agglomerates, the medium crystals are predominantly type A agglomerates, although with a significant proportion of simple crystals, and the large crystals are, almost all, type B agglomerates.

Plotting the size distribution for different values of supersaturation (0.5 m $MgCl_2$), Figure 7, it becomes evident that as the supersaturation increases, the percentage of mainly the large but also of the small crystals decreases. The reason why this happens becomes clear as we analyse Figure 8, where the crystal size distributions for different thermodynamic driving forces are represented.

The population of small crystals is essentially made of simple crystals and type A agglomerates. This population decreases due to crystal growth, increasing the number of

Table 2. Parameters obtained for the growth empirical curves.

Parameters	Obtained results		
	0 m $MgCl_2$	0.5 m $MgCl_2$	1 m $MgCl_2$
k_G ($kg\ m^{-2}\ s^{-1}$)	1.16	0.507	0.226
g	1.885	1.968	1.970

Table 3. Crystal characteristics obtained by image analysis, for $\Delta\mu/RT = 1.375 \times 10^{-3}$ and an impurity concentration of 0.5 m MgCl₂.

	Type A			Type B			Total	
	Simple	Sa	Ma	La	Ka	Kb		Kc
Total number of crystals	104	7	45	146	11	37	21	371
Mean agglomeration degree (%)							55.1	
Mean D_{eq} in number (μm)							615	
Mean D_{eq} in area (μm)							645	
Mean D_{eq} in mass (μm)							662	
Mean D_{eq} – Simple + Type A agglomerates (μm)							579	
CV of number distribution							15.58	
CV of mass distribution							16.51	

medium size crystals. The large crystals are essentially made of type B agglomerates and this type of agglomeration is favoured by low supersaturation values. As the supersaturation increases the proportion of type B agglomerates decreases, making type A agglomerates the predominant kind. This behaviour may also be observed in systems with an MgCl₂ concentration of 1 m.

The effect of the operating conditions on the formation of simple crystals, type A and type B agglomerates was also evaluated. The increase of the impurity concentration did not have a direct influence on the crystal type composition. The impurity affects the growth rate (Figure 5). However, for the same growth rate the crystal type composition is the same. This means that the fraction of each type of crystal in the population is affected by the growth rate and not directly by the impurity concentration.

Analysing Figure 9, one may conclude that the percentage of simple crystals is not changed by the tested operating conditions, but the behaviour differs considering type A and type B agglomerates. The percentage of type A agglomerates increases with the increase of the growth rate, whereas the percentage of type B agglomerates decreases (Figures 10 and 11, respectively). This behaviour explains the decrease in the number of large crystals as supersaturation increases (Figure 7), as pointed out before.

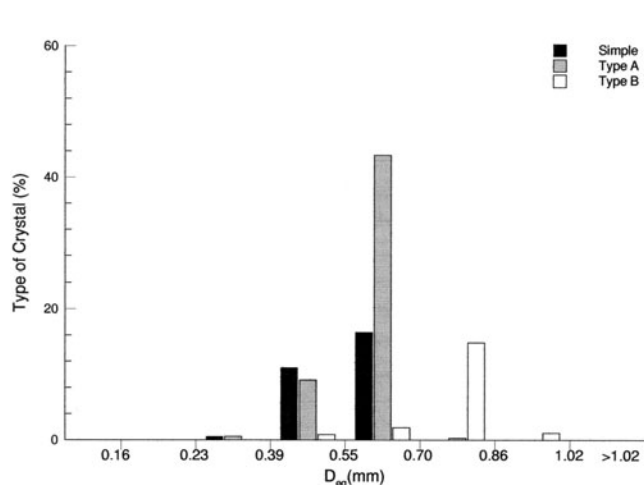


Figure 6. Crystal classification in simple, type A, and type B agglomerate for each size class, for $\Delta\mu/RT = 1.375 \times 10^{-3}$ and an impurity concentration of 0.5 m MgCl₂.

The mean agglomeration degree of the entire population is plotted against the growth rate in Figure 12. Results suggest that the agglomeration degree may be divided in two parts, one for R_g values smaller than $3 \times 10^{-5} \text{ kg m}^{-2} \text{ s}^{-1}$, where coexist the two types of agglomerates, and another for R_g values larger than $3 \times 10^{-5} \text{ kg m}^{-2} \text{ s}^{-1}$, where exist predominantly type A agglomerates.

In the first part the agglomeration degree is reasonably dispersed, whereas in the second part a slight increase of the agglomeration degree with the growth rate can be observed. In general, degree of the agglomeration oscillates between 57% and 70%. The global percentage of agglomerated crystals was also determined and plotted against R_g , (Figure 13). Here, the global percentage of agglomerates oscillates between 70% and 80%, and the average is 76.7%. Apparently, this percentage is not affected by the increase of the impurity concentration.

CONCLUSION

A method for morphology assessment and crystal particle classification has been presented. It is based on combining image analysis with discriminant factorial analysis, leading, after appropriate training, to automated classification within a set structure. The results of this

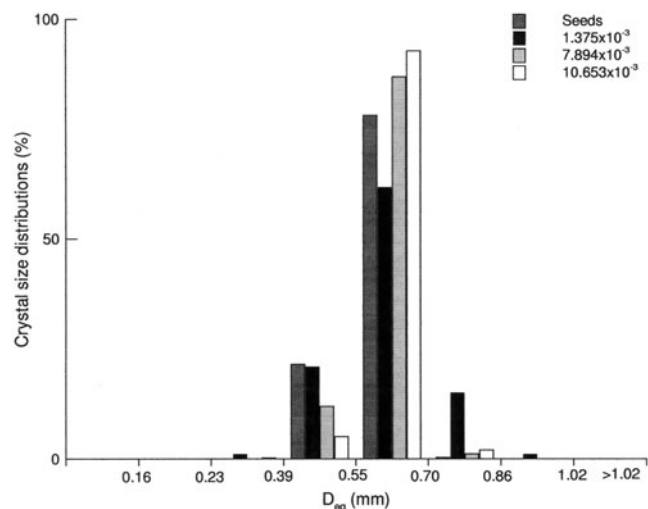
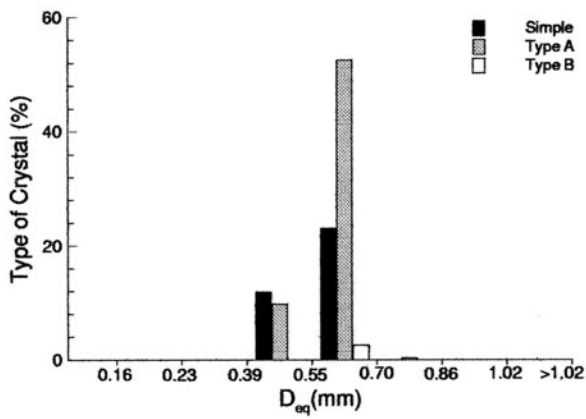
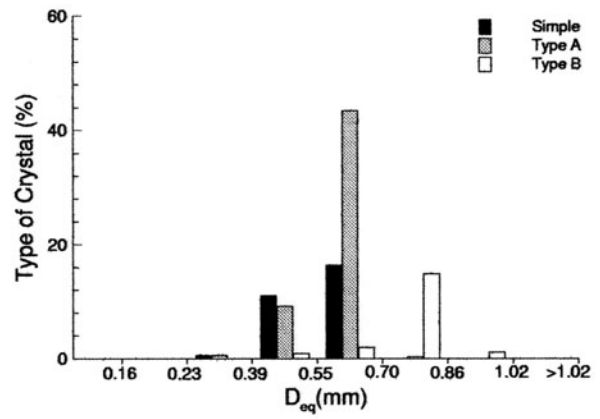


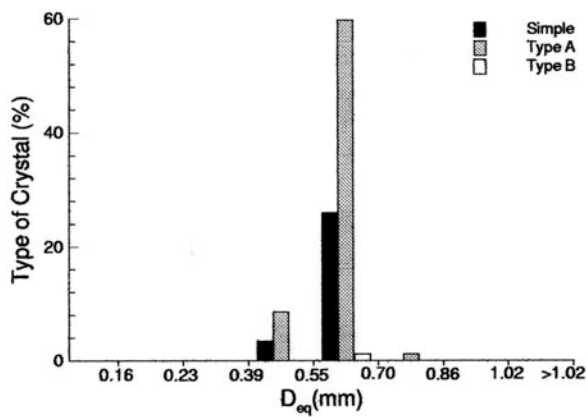
Figure 7. Crystal size distribution for different thermodynamic driving forces and an impurity concentration of 0.5 m MgCl₂.



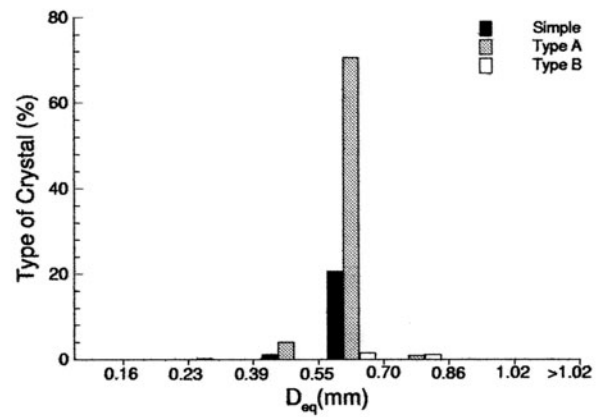
(a)



(b)



(c)



(d)

Figure 8. Crystal classification in simple, type A, and type B agglomerate for each size class: (a) Seeds; (b) $\Delta\mu/RT = 1.375 \times 10^{-3}$; (c) $\Delta\mu/RT = 7.894 \times 10^{-3}$; (d) $\Delta\mu/RT = 10.653 \times 10^{-3}$. Impurity concentration of 0.5 m MgCl₂.

analysis expressed in terms of probabilistic values associated to classes of crystals, further allow the quantification of the complexity level of a crystal or a population of crystals in terms of a new parameter, the agglomeration degree.

The method developed was applied to the study of NaCl crystallization and has proved to be a valuable tool for determining crystal size and morphology. The distinction

between simple crystals and two types of agglomerates (Type A and Type B) was made and the agreement between manual and automated classification, measured in terms of a performance index [equation (7)], is 90% on average. The differentiation of agglomerate sub-classes is not so good due to the higher subjectivity of this last type of classification.

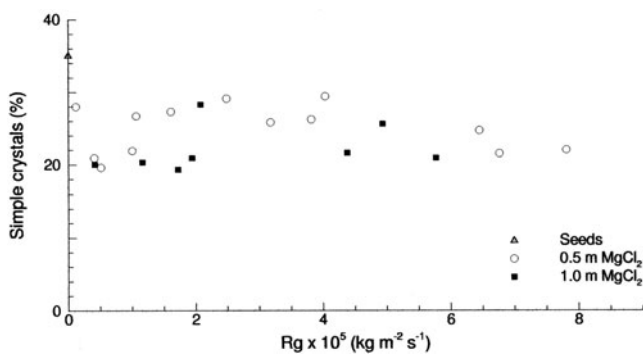


Figure 9. Variation of simple crystals percentage with crystal growth rate for different impurity concentrations.

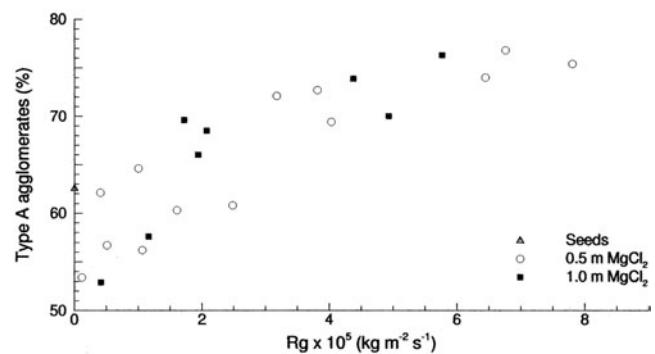


Figure 10. Variation of type A agglomerates percentage with crystal growth rate for different impurity concentrations.

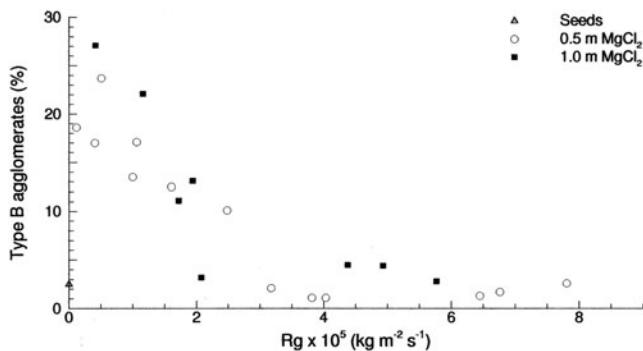


Figure 11. Variation of type B agglomerates percentage with crystal growth rate for different impurity concentrations.

The further use of this method on the study of NaCl crystallization under different operation conditions showed to be very useful. The effect of the supersaturation and the impurity concentration on the type of crystals and agglomeration degree was studied. It is verified that this effect can be explained solely as a function of growth rate, that is, different experimental situations, but having the same growth rate, will lead to the same effect in the measured properties.

For low growth rates type B agglomerates are predominant and their proportion decreases with the increase of growth rate. The opposite happens with the type A agglomerates. This suggests that type B agglomerates may indeed be formed by a phenomenon closer to aggregation, whereas type A agglomerates would be 'pure' agglomerates according to the definition presented in the Introduction. However, more experimental evidence would be needed to make a clear statement on this issue.

The percentages of simple crystals and agglomerates remain practically constant under different operating conditions (around 23% and 77%, respectively).

The behaviour of the agglomeration degree with the growth rate is not uniform. For low growth rates the agglomeration degree seems to be constant although rather scattered, whereas for higher growth rates it exhibits a tendency for increasing. This behaviour is directly related to the fact that the complexity of agglomerates A and B

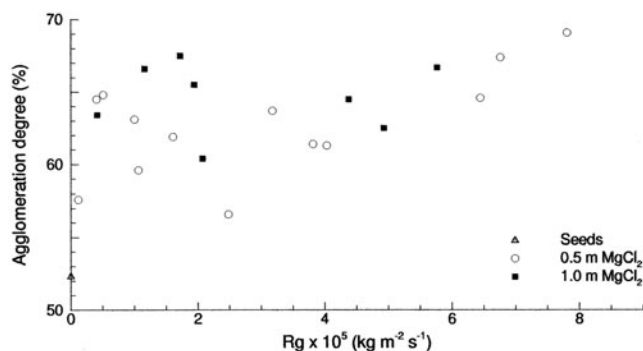


Figure 12. Variation of mean agglomeration degree with crystal growth rate for different impurity concentrations.

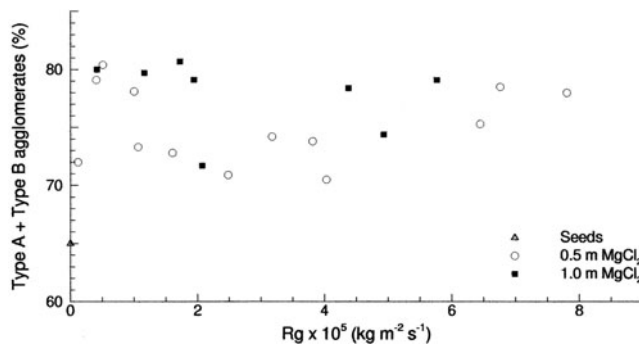


Figure 13. Variation of type A + type B agglomerates with crystal growth rate for different impurity concentrations.

is mixed in the calculation of the agglomeration degree and reveals the dangers of disregarding the morphology of agglomerates in the study of NaCl agglomeration mechanisms.

REFERENCES

- Faria, N., Pons, M.N., Fayo de Azevedo, S., Rocha, F. and Vivier, H., 2003, Quantification of the morphology of sucrose crystals by image analysis, *Powder Technology*, 133: 54–67.
- Ferreira, A. and Lopes, A., 2002, A new potentiometric method to evaluate supersaturation in aqueous systems, in Chinese, A. (ed.), *Proceedings of 15th International Symposium on Industrial Crystallization*, AIDIC, Sorrento, Italy, 137–142.
- Fayo de Azevedo, S., Rocha, F., Faria, N. and Pons, M.N., 2002, Using image analysis to look into the effect of operating conditions in sugar crystallisation, in Chinese, A. (ed.), *15th International Symposium on Industrial Crystallization*, AIDIC, Sorrento, Italy, 1377–1382.
- Hartel, R., Gottung, B.E., Randolph, A.D. and Drach, G.W. 1988, Mechanisms and kinetic modelling of calcium oxalate crystal aggregation in a urinelike liquor. I. Mechanisms. *AIChE J*, 32: 1176–1185.
- Mersmann, A., 1994, *Crystallization Technology Handbook*, (Marcel Dekker, New York, USA).
- Mullin, J.W., 1992, *Crystallization*, 3rd edition (Butterworth-Heinemann, Oxford, UK).
- Perry, L.R. and Green, D., 1984, *Perry's Chemical Engineer's Handbook*, 6th edition (McGraw-Hill, New York, USA).
- Pitzer, K., 1995, *Thermodynamics*, 3rd edition, (McGraw-Hill, New York, USA).
- Pons, M.N., Camarasa, E., Vivier, H., Faria, N., Rocha, F. and Fayo de Azevedo, S., 1998, Shape characterisation of sugar crystals, *Proceedings of World Congress of Powder Technology*, number 33, World Congress of Powder Technology, Brighton (IChemE, Rugby, UK).
- Pons, M.N., Vivier, H. and Dodds, J. 1997, Particle shape characterization using morphological descriptors. *Part Part Syst Charact*, 14: 272–277.
- Puthela, R., Pitzer, K. and Saluja, P., 1987, Thermodynamics of aqueous magnesium chloride, calcium chloride, and strontium chloride at elevated temperatures. *J Chem Eng Data*, 32: 76.
- Schubert, H., 1981, Principles of agglomeration, *Int Chem Eng*, 21: 363–377.

ACKNOWLEDGEMENTS

This work was partially developed in the Laboratories of the Research Unit Instituto de Sistemas e Robótica, Porto, and partially financed by Fundação para a Ciência e Tecnologia, the National Foundation for Science and Technology, Contract POCTI/33131/EQU/2000.

The manuscript was received 11 May 2004 and accepted for publication after revision 19 January 2005.